ACS OMEGA

Open Access

This article is licensed under CC-BY-NC-ND 4.0

http://pubs.acs.org/journal/acsodf

Article

Electrical Contacts to Graphene by Postgrowth Patterning of Cu Foil for the Low-Cost Scalable Production of Graphene-Based Flexible Electronics

Lee Kyung Bae, Seong Gyun Son, Sang-Chan Park, Won Gyun Park, Kiwan Kim, Hyo-Ju Lee, Daeun Bang, Su-Ho Cho, Il-Suk Kang, and Jae-Hyuk Ahn*

Cite This: *ACS Omega* 2025, 10, 1448−1456

Read Online

ACCESS | Metrics & More | Article Recommendations | Supporting Information

ABSTRACT: Numerous studies have focused on graphene owing to its potential as a next-generation electronic material, considering its high conductivity, transparency, superior mechanical stiffness, and flexibility. However, cost-effective mass production of graphene-based electronics based on existing fabrication methods, such as graphene transfer and metal formation, remains a challenge. This study proposes a simple and efficient method for creating electrical contacts with graphene. The method involves patterning a Cu foil after graphene growth, enabling the low-cost scalable production of graphene-based flexible electronics. The fabricated graphene devices exhibited linear current−voltage characteristics, indicating good electrical contact between the postgrowth-patterned Cu electrodes and graphene. The proposed postgrowth patterning method allows for the fabrication of Cu-contacted graphene devices on large areas and various flexible substrates, including ultrathin and stretchable films (<10 μm). The feasibility of the proposed method for electronic devices was demonstrated by implementing gas and flexible force sensors. The proposed approach advances the field of graphene-based electronics and holds potential for practical applications in various electronic devices, paving the way for scalable, cost-effective, and flexible technology solutions.

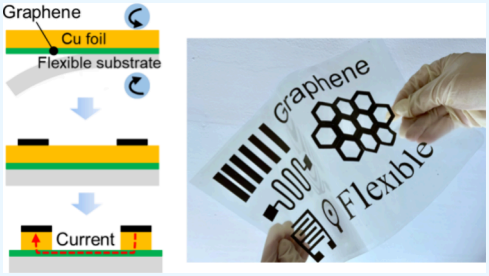

INTRODUCTION

Graphene, a honeycomb-like sheet of carbon atoms, has gained significant research attention owing to its potential as a next-generation electronic material with diverse applications, considering its high conductivity, transparency, superior mechanical stiffness, and flexibility.[1−4] Since the discovery of graphene sheets through the mechanical exfoliation of graphite in 2004,[1] various preparation methods of graphene have been developed, such as liquid-phase exfoliation,[5,6] desorption of Si from SiC single-crystal surfaces,[7,8] and chemical vapor deposition (CVD).[9−11] Among these, the CVD method produces high-quality large-area graphene films on Cu foils, reaching sizes of centimeters or meters,[12,13] As a self-limited process facilitated by the low solubility of carbon in Cu, CVD enables scalable production of large-area monolayer graphene without adlayers (i.e., bilayer or multilayer regions),[14,15] a crucial requirement for industrial applications of graphene-based electronics. CVD-grown graphene on Cu foil is typically processed into graphene-based electronics through two fabrication steps: graphene transfer and electrode formation. Graphene film is then transferred to a target substrate, usually with an insulating layer. The wet transfer method with a carrier layer (i.e., a polymer) coated on CVD-grown graphene is commonly used owing to its advantage in maintaining the integrity of the graphene film.[16−18] The polymer/graphene stack is transferred to the target substrate after etching the growth substrate (i.e., Cu foil) with a liquid etchant. The graphene-coated substrate is completed by removing the polymer. Details of the transfer methods are provided in review papers.[19,20] After the graphene transfer process, metal electrodes are formed on the graphene-coated substrate for electrical contacts with graphene by combining photolithography and metal deposition processes, such as evaporation and sputtering.[21−23] Various attempts at Cu recycling have been made for graphene transfer.[24−27] A mechanical peeling method called "dry transfer"[24,25] and electrochemical process called "bubbling transfer" using hydrogen bubble generated during water electrolysis process[26,27] delaminate the graphene from the Cu foil without etching, enabling Cu substrate reuse. Various studies have demonstrated the direct growth of graphene on target substrates, such as SiO_2,[28,29] polyimide (PI),[30,31] and polyethylene terephthalate (PET).[30,32]

However, achieving low-cost, scalable fabrication of metal electrodes on flexible substrates for graphene-based electronics

Received: October 7, 2024
Revised: December 14, 2024
Accepted: December 16, 2024
Published: December 23, 2024

© 2024 The Authors. Published by American Chemical Society

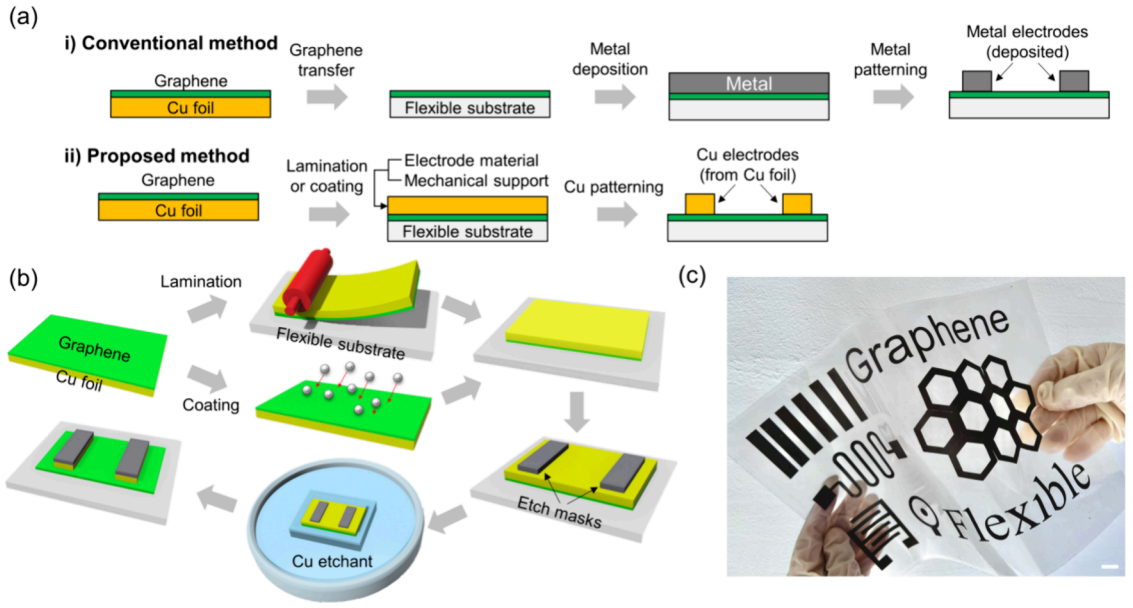

Figure 1. Electrical contacts to graphene using postgrowth-patterned Cu foil. (a) Comparison of electrical contacts between the conventional and proposed methods for fabricating graphene-based flexible electronics. In the conventional method, a Cu foil (i.e., the growth substrate of CVD-grown graphene) is completely etched (or delaminated) for graphene transfer, and metal is deposited on the graphene for electrical contacts. In the proposed approach, the Cu foil is used as an electrode to create an electrical contact with graphene by patterning the Cu foil into the desired electrode shape without additional metal deposition on the graphene. (b) Schematic of the fabrication process of electrical contacts with graphene using postgrowth-patterned Cu foil. (c) Graphene-based flexible device with postgrowth-patterned Cu electrodes fabricated on a 12.9-in. silicone/PET film. Scale bar: 1 cm. Photograph courtesy of "Lee Kyung Bae". Copyright 2024. Reusing the image needs permission.

remains challenging. Metal deposition processes require the operation of large vacuum equipment and the consumption of metal sources, potentially increasing the cost of disposable graphene sensors, such as patches and tattoos.[33−36] In addition, ultrathin and stretchable substrates, prone to wrinkling or curling,[37−39] require additional processing steps, such as attaching the flexible substrate to a handling substrate and lift-off (or delamination) of the substrate after the completion of fabrication,[40−42] potentially affecting the production cost.

This study proposes the concept of creating electrical contacts with graphene by patterning a Cu foil after graphene growth for the low-cost scalable production of graphene-based flexible electronics. Rather than implementing additional metal deposition, Cu foil, a graphene growth substrate, was used as the metal electrode. A flexible substrate was covered with a graphene film synthesized on a Cu foil, and the Cu foil was patterned into individual electrodes through Cu etching with masking layers. Combining large (up to 12.9 in) graphene/Cu films and a "cut-and-paste" method of masking materials onto the Cu foil yielded a scalable array of graphene devices on a flexible substrate. The proposed approach leverages a copper substrate to facilitate a cost-effective and efficient method for patterning graphene without the necessity of additional metal deposition, thereby distinguishing it from existing research that primarily focuses on synthesis and transfer techniques.[12] The Cu-contacted graphene devices exhibited linear current−voltage (I−V) characteristics, indicating good electrical contact between the Cu foil and graphene. The contact resistance between the Cu-based contacts and graphene was determined using a test pattern at various distances. The proposed postgrowth patterning of Cu foil was applied to various flexible materials, including ultrathin stretchable films, such as silicone/PET, thermal release tape (TRT), polydimethylsiloxane (PDMS) film, PI tape, parylene, and polyurethane (PU). Electrical contacts to graphene created through the postgrowth patterning of Cu foil were used to implement gas sensors for detecting NH_3 and NO_2 gases and flexible force sensors capable of responding to bending tests.

RESULTS AND DISCUSSION

Proposed Concept: Electrical Contacts with Graphene by Postgrowth Patterning of Cu Foil. In conventional methods for fabricating graphene-based electronics (Figure 1a, left), CVD-grown graphene on a Cu foil is transferred to a target substrate by etching or delaminating the Cu foil. Subsequently, metal evaporation or sputtering is performed to form metal electrodes on the graphene. In the proposed approach (Figure 1a, right), the additional process of metal deposition is eliminated by utilizing the Cu foil (i.e., growth substrate) as electrical contacts or electrodes for graphene. The proposed method does not require metal sources and vacuum equipment used in metal deposition, reducing process costs and simplifying fabrication.

Gold is commonly used as an electrode but does not support in situ graphene growth through chemical vapor deposition (CVD), requiring instead complex transfer processes from other substrates.[43] Copper, by contrast, allows direct CVD-based graphene growth, simplifying fabrication and enhancing electrode stability and performance, making it highly suitable for scalable, cost-effective graphene-based applications.[12,44,45]

Figure 1b shows the fabrication process of graphene devices through the postgrowth patterning of the Cu foil. The top side of the graphene on the Cu foil was covered with a silicone/PET film, and the back side was etched through an O_2 plasma process (100 W for 90 s). The flexible substrate used in this study is a silicone/PET composite, with a silicone layer added to improve PET's thermal stability and insulation, making it

https://doi.org/10.1021/acsomega.4c09156
ACS Omega 2025, 10, 1448−1456

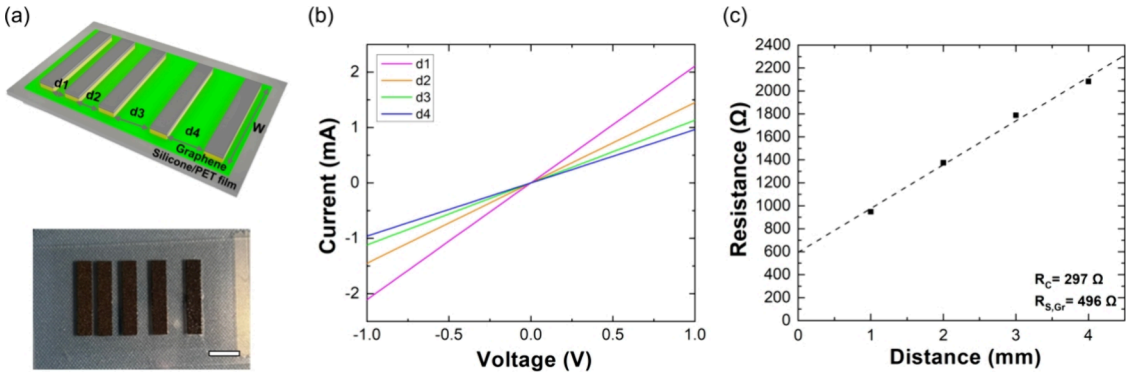

Figure 2. Electrical characteristics of postpatterned Cu contacts. (a) Schematic (top) and optical image (bottom) of the test pattern with various spacing distances for determining the contact and sheet resistances. A CVD-grown graphene on a silicone/PET film was electrically contacted with the postgrowth-patterned Cu electrodes at various distances. Scale bar: 1 cm. Photograph courtesy of "Lee Kyung Bae". Copyright 2024. Reusing the image needs permission. (b) Current−voltage characteristics. (c) Resistance versus distance.

more suitable for applications involving temperature variations. Although not illustrated here, the top graphene layer on the Cu foil could be patterned to define the active area using an etching mask through O_2 plasma etching. The thin film of the Cu foil was transformed into Cu electrodes through a conventional patterning process: placing etch masks and etching with a Cu etchant (0.3 M APS solution for 90 min). Cu-contacted graphene devices can be fabricated using different masking materials, categorized as nonconducting or conducting materials (Table S1). Conductive carbon tape was selected as the masking material owing to its suitability for economical and large-scale processes. In this study, conductive carbon tape was securely adhered to the copper foil, ensuring no infiltration of APS solution during the etching process. The strong adhesion of the tape effectively prevented solution seepage, maintaining precise etching boundaries, and ensured minimal contact resistance, allowing reliable electrical performance measurements. However, it is worth noting that the conventional photolithography process using a photoresist can be employed to achieve high-resolution patterning if required (Figure S1).

Figure 1c shows an example of the fabricated Cu-contacted graphene device. An array of graphene devices was fabricated on a flexible substrate (silicone/PET film) with an area of up to 12.9 in. This configuration demonstrates the feasibility of using Cu foil as a growth substrate and an electrode material, showcasing its potential for flexible electronics where cost efficiency and process simplicity are essential.

Electrical Characteristics of Cu Foil-Based Contacts. The electrical characteristics of the Cu-contacted graphene devices were evaluated by determining the contact resistance between Cu and graphene. A test pattern with various distances between the Cu electrodes was used (Figure 2a,b). This method, known as the transfer length method (TLM), is widely used for determining the contact resistance of graphene device.[46,47] The graphene was patterned via an O_2 plasma etching process to define the active area and ensure accurate TLM measurements. The top graphene layer on the Cu foil was covered with a patterned carbon mask, and the Cu foil was subsequently etched using a Cu etchant. This patterning process is crucial to isolate individual graphene channels and minimize measurement errors associated with unpatterned sheets. The equation, $R_{tot} = 2R_C + R_{S,Gr}(d/W)$, was used, where R_C, $R_{S,Gr}$, d, and W denote the contact resistance between the Cu-based contact and graphene, graphene sheet resistance, distance between the contacts, and width of the graphene channel, respectively. The fabricated graphene devices exhibited linear $I-V$ characteristics (Figure 2b), indicating good electrical contact between the Cu substrate and graphene. The distance between the Cu electrodes influence the resistance values (Figure 2c). From the linear fitting of the resistance (R) as a function of distance (d), the calculated contact resistance of Cu/graphene and sheet resistance of graphene were 297 Ω (386 Ω mm) and 496 Ω/□, respectively. The contact resistance of the Cu/graphene device is similar to the values (∼100 Ω mm) of the contact resistance between graphene and other metal contacts (Ti, Ti/Au, and Cr/Au).[48] The contact resistance of the proposed device is relatively high, which makes the proposed Cu/graphene contacts unsuitable for high-performance transistor applications. Acknowledging this limitation, the focus has shifted to the cost-effective fabrication of disposable sensors. The total resistance of graphene sensors is expressed as $R_{tot} = 2R_C + R_{Gr}(d/W)$. The graphene sensor should be designed with $R_{GR}(d/W)$ larger than R_C, effectively allowing for the measurement of a change in the graphene channel resistance when subjected to an external stimulus.

The graphene-Cu-graphene configuration not only effectively isolates the copper foil from environmental oxygen, thereby preventing oxidation, but also significantly enhances the electrical conductivity and durability of the contacts. This encapsulation reduces the contact resistance, critical for high-performance applications, as demonstrated by the improved interface quality in our SEM, Raman spectroscopy, and XPS analyses.[49] Furthermore, CVD-grown graphene provides robust protection for Cu surfaces against oxidation at elevated temperatures, ensuring long-term stability and reliability under operational conditions.[50] Additionally, thicker copper foil may improve oxidation resistance, potentially extending device lifetime by minimizing surface degradation. This phenomenon has been observed in previous studies where increased copper thickness led to enhanced stability against oxidation, especially in high-temperature or reactive environments.[51] Therefore, using thicker copper foil in our proposed device could further stabilize contact resistance over prolonged operational periods, supporting its application in disposable sensors and other flexible electronic devices.

Postgrowth Patterning of Cu Foil Applied to Various Flexible Materials. The proposed postgrowth patterning method can be applied to various flexible substrate materials.

https://doi.org/10.1021/acsomega.4c09156
ACS Omega 2025, 10, 1448−1456

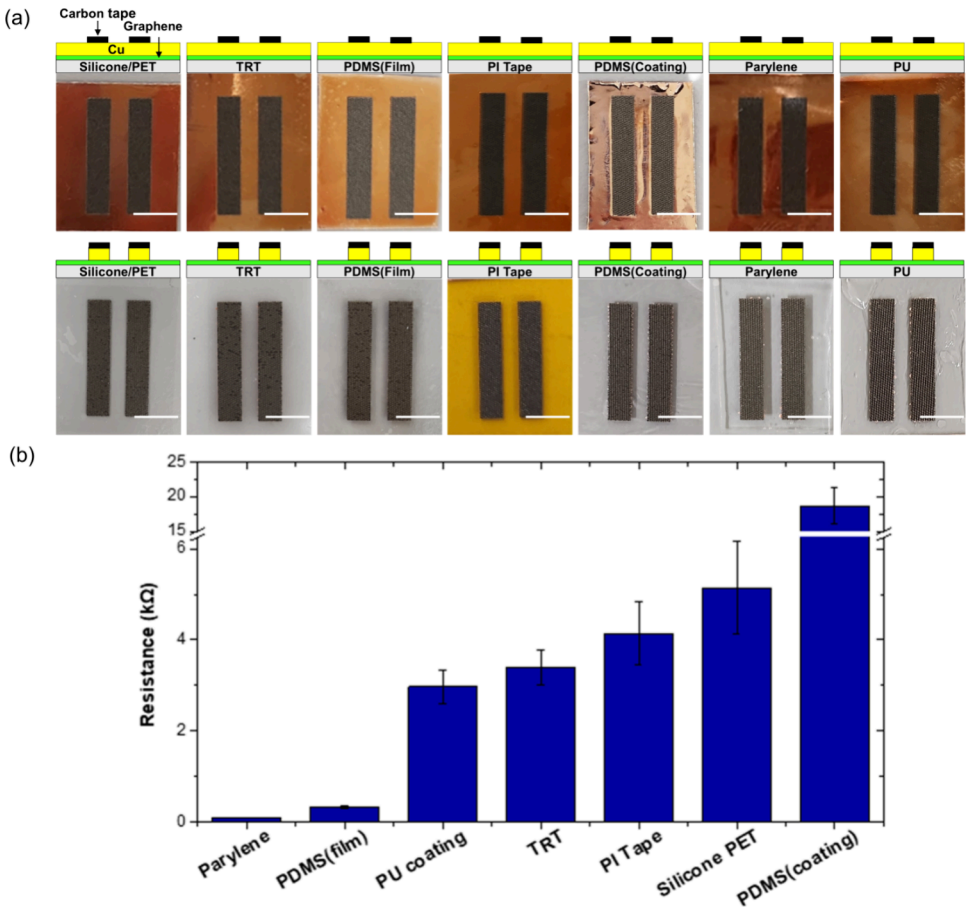

Figure 3. Postpatterning of Cu foil on various flexible substrates. (a) Optical images of the graphene devices on different flexible substrates before (top) and after (bottom) postpatterning of the Cu foil. Scale bar: 1 cm. Photograph courtesy of "Lee Kyung Bae". Copyright 2024. Reusing the image needs permission. (b) Resistance values for the Cu-contacted graphene devices with various flexible substrates.

CVD-grown graphene on Cu foil was attached to flexible substrates using two different methods: (1) lamination of graphene/Cu foil with a flexible substrate and (2) coating of a precursor polymer onto graphene/Cu foil through spin-coating or CVD. The detailed processes for preparing the multilayer structures of the flexible substrate/graphene/Cu foil are described in the Supporting Information (Figure S2) or Methods. Figure 3a shows the postgrowth patterning of the Cu foil applied to laminated substrates, such as silicone/PET, TRT, and PDMS films. These flexible substrates have sufficient adhesion suitable for graphene attachment and adequate thickness (>100 μm) for mechanical handling during fabrication. The direct lamination of graphene/Cu foil onto these flexible substrates is compatible with roll-to-roll processing,[52,53] facilitating industrially scalable production of graphene-based electronics. The postgrowth patterning method was also applied to graphene/Cu foil coated with polymer thin films, such as parylene and PU (Figure 3a). These ultrathin and stretchable films are too thin (<10 μm) to handle mechanically, requiring attachment of the film on a handling substrate with a sacrificial layer and the subsequent lift-off process after fabrication.

However, in the postgrowth patterning method, the Cu foil serves as a handling substrate to mechanically support the graphene and ultrathin polymer film, enabling patterning without additional attachment and lift-off processes.

Figure 3b shows the resistance values of the graphene devices (Figure 3a) on various flexible substrates. All devices exhibited linear $I-V$ characteristics (Figure S3), confirming that current flowed between the Cu electrodes through the graphene channel. Flexible substrates can be fabricated using the lamination and coating methods. The resistance of graphene-based devices varies based on the substrate material. The interfacial material affects the conductivity of graphene. Interfacial defects that deteriorate device performance may occur at the interface between the graphene and substrate material. If the trapped charge occupies the majority of the moving charge in the graphene channel, and the recharging process is repeated, the change in the Fermi energy is significantly hindered, degrading performance.[54] Applying various substrate materials to graphene is beneficial for identifying substrates with excellent interfacial properties. Specifically, the higher currents observed on parylene can be attributed to its superior insulating properties and excellent compatibility with high-quality graphene. This compatibility improves electron mobility by forming a high-quality interface with graphene, thereby enhancing device performance.[55] Compared to PDMS film, devices formed on PI and PU films exhibit lower currents owing to their higher dielectric constants and greater charge scattering, which reduce electron mobility.[56] The excellent flexibility, low dielectric constant, and high chemical resistance of PDMS make it more suitable for maintaining the integrity of the graphene layer and facilitating better charge transport.[57]

Application (1): Gas Sensors. The ability of the postgrowth-patterned Cu contacts to detect changes in the

https://doi.org/10.1021/acsomega.4c09156
ACS Omega 2025, 10, 1448−1456

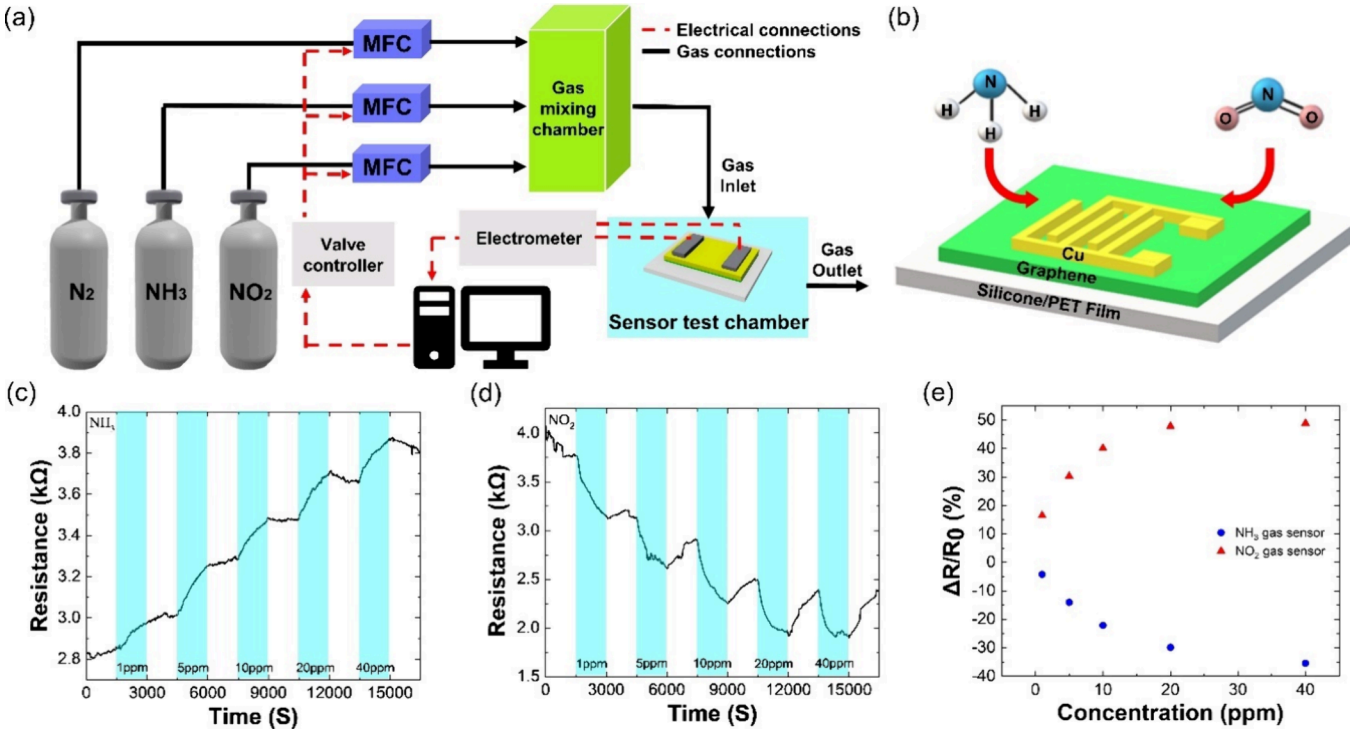

Figure 4. Gas sensing using graphene devices with postpatterned Cu contacts. (a) Schematic of the gas test setup. (b) Schematic of the interaction between the gas molecules (NH_3 and NO_2) and graphene device. (c) Resistance versus NH_3 concentration. (d) Resistance versus NO_2 concentration. (e) Normalized resistance versus gas concentration.

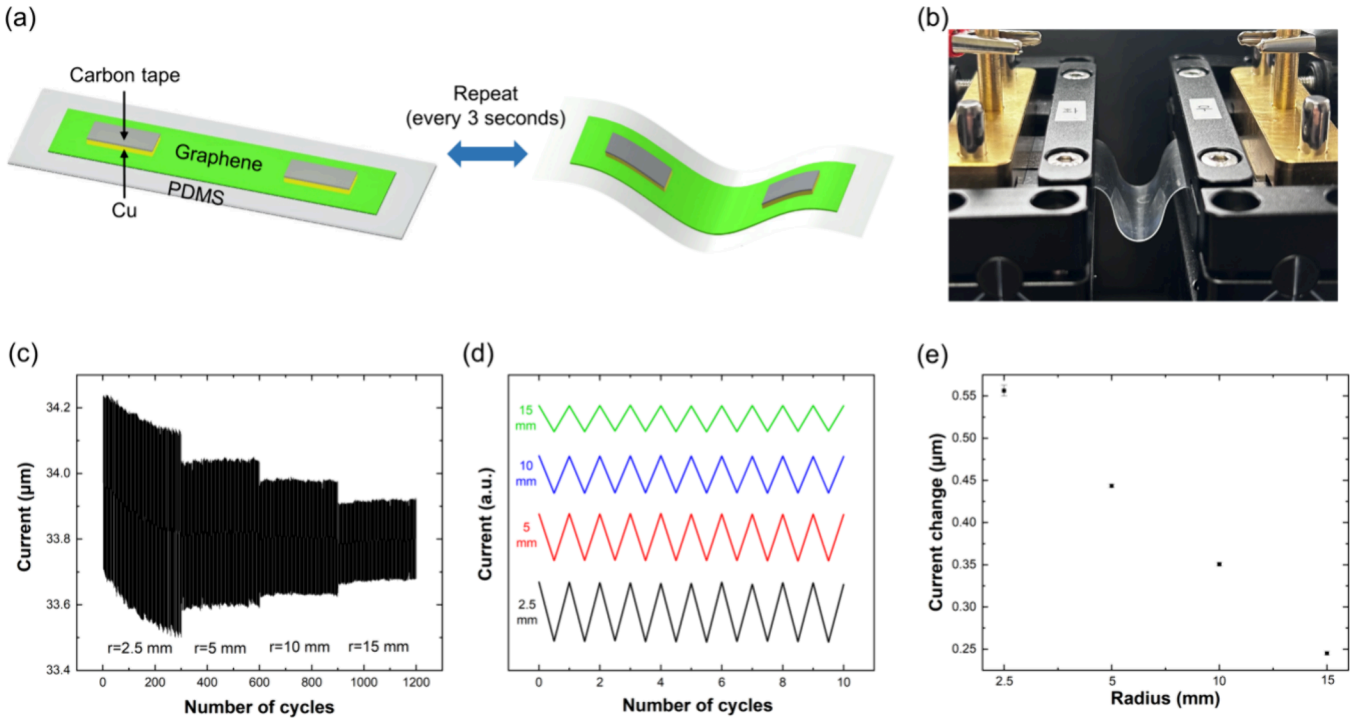

Figure 5. Bending test of graphene devices with postpatterned Cu contacts. (a) Schematic of the bending test procedure. (b) Optical image of the bending test setup. Photograph courtesy of "Lee Kyung Bae". Copyright 2024. Reusing the image needs permission. (c) Current versus time curves for repetitive bending with bending radii (r) of 2.5, 5, 10, and 15 mm. (d) Magnified waveforms of the bending profiles at different bending radii. (e) Change in current versus r. The error bars represent the average difference in current between contraction and relaxation phases over ten cycles, using the values from Figure (d) for each bending radius.

signal (i.e., resistance) from graphene-based sensors was evaluated. Gas-sensing experiments were performed using graphene devices and postgrowth-patterned Cu contacts (Figure 4a,b). The resistance of graphene increased upon exposure to NH_3 gas (Figure 4c). By contrast, exposure to NO_2 gas reduced the resistance of graphene (Figure 4d). The

https://doi.org/10.1021/acsomega.4c09156
ACS Omega 2025, 10, 1448−1456

graphene devices exhibited concentration-dependent resistance changes for NH_3 and NO_2 gases (Figure 4e). The similar response trends for NO_2 and NH_3 gases are likely caused by the intrinsic electronic properties of CVD-grown graphene, which exhibits high sensitivity to both electron donor and acceptor gases under specific conditions.[58] Additionally, the Cu electrode plays a catalytic role in enhancing the gas sensor response.[59] When NH_3 molecules adsorb onto the Cu surface, they participate in reduction reactions, releasing electrons that subsequently increase the resistance in the graphene layer by reducing charge mobility.[60]

Conversely, NO_2 molecules on the Cu surface undergo oxidation, accepting electrons that lower the resistance in the graphene.[61] This catalytic activity of the Cu electrode accelerates electron transfer rates, enhancing the sensitivity and response time of the sensor for low-concentration gases.[62] These experimental results align well with previous studies on graphene-based gas sensors, where exposure to NH_3 increases resistance and NO_2 decreases it, as illustrated in Figure 4c,d.[63,64] Upon stopping the NO_2 gas flow, the sensor gradually returns to its baseline resistance due to the desorption of NO_2 molecules from the graphene surface.[65] While recovery remains incomplete, additional energy sources like high temperatures or light can facilitate the desorption process.[66,67] Gas sensing signals primarily originate from the Cu/graphene contacts, where the Cu layer's catalytic properties enhance detection capabilities by promoting faster electron transfer rates and improving sensitivity and response time for low-concentration gases.[68−71] To ensure accurate evaluation of sensor response, the gas sensing experiments were conducted under controlled environmental conditions, including humidity, temperature, and airflow, to minimize the influence of external factors on sensor performance. The high gas flow rate of 1000 sccm was maintained to allow rapid and consistent replacement of the testing atmosphere, ensuring reproducible sensor measurements.

Application (2): Flexible Force Sensors. The electrical characteristics of the postgrowth-patterned electrodes in a graphene-based sensor was evaluated through mechanical bending. The process involved repeated mechanical contraction and relaxation upon application of external forces. The bending test was performed by measuring the current values based on the bending radius (r) as the Cu-contacted graphene device using a PDMS substrate was bent (Figure 5a). As r decreased or the degree of bending increased, a significant difference in the current values was observed when the substrate contracted and relaxed (Figure 5c,d). Bending the substrate more significantly increased the stress on the device, resulting in a larger change in current (Figure 5e). The flexible Cu-contacted graphene devices demonstrated applicability in electronic skins,[72,73] responding to mechanical stimuli. The mechanical deformation of graphene caused by bending the device alters the electronic band structure of graphene, which affects the mobility of charge carriers, resulting in variations in the current.[74] In addition, the strain sensing mechanisms of graphene-based flexible sensors primarily originate from the geometrical effect and the piezoresistive effect of the graphene material.[72] The mechanoelectrical transduction properties observed in our bending tests validate the potential of these sensors for practical force sensing applications. When subjected to mechanical bending, the induced strain changes the electrical properties of graphene-based sensors, specifically their resistance. This strain-induced change in resistance is a direct measure of the mechanical force applied to the sensor, thereby demonstrating the capability of the sensor to detect and measure force.

CONCLUSIONS

This study demonstrated the concept of postgrowth patterning of Cu foil, enabling the formation of electrical contacts with CVD-grown graphene by utilizing the Cu foil as the electrode material. The postgrowth patterning method involved etching of the Cu foil into desired electrode patterns using a masking layer (i.e., conductive carbon tape), applied on the Cu foil/graphene/flexible substrate through a simple "cut-and-paste" method. The proposed approach enables the cost-effective production of graphene devices by eliminating the metal deposition process used in conventional approaches. Moreover, it facilitates scalable fabrication of a large-area device array on a flexible substrate approximately the size of the Cu foil. The Cu-contacted graphene devices exhibited nonrectifying linear $I-V$ characteristics with a contact resistance of 445.5 Ω mm. The proposed postgrowth patterning method proved to be a universal method applicable to various flexible substrates, such as silicone/PET, TRT, PDMS, parylene, and PU. In this approach, the Cu foil functions as an electrode material and a mechanical support. This allows for the formation of electrodes on ultrathin and stretchable films, which are typically difficult to manipulate without proper handling of the substrate. The Cu-contacted graphene devices were applied for gas and force sensing applications. The postgrowth patterning of Cu foil is a promising fabrication method for achieving low-cost scalable production of graphene-based electronics for flexible and disposable sensors.

METHODS

Materials. CVD-grown monolayer graphene sheets on Cu foil (thickness = 18 μm) were purchased from Charmgraphene Co., Ltd. (South Korea). Ammonium persulfate (APS) (248614) was purchased from Sigma-Aldrich (United States). A commercial screen protector (silicone/PET film) for iPad Pro 12.9-in. was purchased from Skoko (South Korea). Thermal release tape (TRT) was purchased from Jinsung Chemicals Co., Ltd. (South Korea). A 200 μm thick polydimethylsiloxane (PDMS) film was purchased from CSCRIE Co., Ltd. (Japan). A 70 μm thick PI adhesive tape was purchased from iNexus, Inc. (South Korea). The PDMS base and curing agent were purchased from Dow Corning (United States). A conductive carbon tape (EST12250) with a width of 50 mm was purchased from LK Lab Korea (South Korea).

Multilayer Structures of Flexible Substrate/Graphene/Cu Foil. Two methods were employed in preparing a multilayer flexible substrate/graphene/Cu foil: (1) lamination of the graphene/Cu foil with a flexible substrate and (2) coating of a precursor polymer onto the graphene/Cu foil. The CVD-grown monolayer graphene sheet on the Cu foil was laminated onto a flexible substrate, such as a silicone/PET film, TRT, adhesive PI tape, and PDMS film, using a laminator. Subsequently, O_2 plasma etching (100 W for 90 s) was performed to remove the back-side graphene on the Cu foil. For the coating process, a PDMS elastomer mixed with an elastomer base and a curing agent at a ratio of 10:1 was cured onto the graphene/Cu foil and heated at 150 °C for 15 min on a hot plate. To prepare the ultrathin polymer film, a 1 μm thick

https://doi.org/10.1021/acsomega.4c09156
ACS Omega 2025, 10, 1448−1456

parylene C was coated onto the graphene/Cu foil through CVD. Subsequently, O_2 plasma etching (100 W for 90 s) was performed to remove the back-side graphene on the Cu foil. To prepare the ultrathin and stretchable films, a tetrahydrofuran (THF)-based solution with a PU pellet (5%) was spin-coated onto the graphene/Cu foil at a rate of 1,000 rpm at room temperature. These ultrathin and stretchable substrates attached to the Cu foil can be mechanically handled for device fabrication without an additional supporting substrate.

Postgrowth Patterning of Cu Foil. The postgrowth Cu foil was patterned into electrodes in two steps: (1) gorming a masking layer on the Cu foil/graphene/flexible substrate and (2) Cu etching. The conductive carbon tape used as a masking material was cut into electrode shapes using a computer-controlled CO_2 laser (Universal Laser Systems VLS 2.30DT) with a power of 20 W and scan rate of 20 in/s. After peeling off the unwanted carbon tape from the release liner, the designed mask patterns of the adhesive carbon tape were laminated onto the Cu foil/graphene/flexible substrate. This is similar to the "cut-and-paste" method for the rapid prototyping of soft electronics.[75] The formation of masking patterns with additional materials is presented in the Supporting Information. A 0.3 M ammonium persulfate (APS) solution was used to remove the Cu foil unprotected by the masking patterns, forming separate Cu electrodes in contact with graphene. The removal of the carbon tape masking patterns on the Cu electrodes can be omitted for the electrical characterization of the fabricated graphene devices because the carbon tape is highly conductive (0.3 Ω/□).

Gas Sensing. The electrical characteristics of the Cu-contacted graphene devices were measured using a semiconductor parameter analyzer to verify the electrical reaction between the graphene and gases (NO_2 and NH_3) over time. After placing the postgrowth-patterned Cu contacts in the gas test chamber, the concentration of NO_2/NH_3 gas was gradually increased from 1 to 40 ppm (1, 5, 10, 20, and 40 ppm) (Figure 4a). The total gas flow rate was fixed at 1000 sccm. The gas injection and N_2 purging were alternated at 25 min intervals. The high flow rate of 1000 sccm helps achieve rapid response times by quickly replacing the gas around the sensor, ensuring the sensor quickly reaches a steady state when exposed to different gas concentrations. Additionally, the high flow rate ensures consistent gas concentration throughout the sensing chamber and contributes to the reproducibility of sensor measurements, resulting in reliable and reproducible sensor performance.[76]

Bending Test. The bending tests involved measuring the resistance change of the Cu-contacted graphene devices using a PDMS substrate through repeated contraction and relaxation. After fixing the postgrowth-patterned Cu contacts in a motion controller (ST-BJS-0810-SSU, Koreaopto (South Korea)), the electrical properties were measured using a SourceMeter (Keithley 2612 B) by varying the radius (r) of the bent portion to 2.5, 5, 10, and 15 mm using a motion controller (STM-1-TS, ST1 (South Korea). The contraction and relaxation were performed 300 times for each radius.

■ ASSOCIATED CONTENT

Data Availability Statement

Data supporting the findings of this study are available from the corresponding author upon request.

Supporting Information

The Supporting Information is available free of charge at https://pubs.acs.org/doi/10.1021/acsomega.4c09156.

Additional experimental details, methods, and results (DOC): Selection of masking materials; postgrowth patterning of Cu foil using photolithography; fabrication processes for the postgrowth patterning of Cu foil; and $I-V$ characteristics of the Cu-contacted graphene devices applied to various flexible materials (PDF)

■ AUTHOR INFORMATION

Corresponding Author

Jae-Hyuk Ahn − *Department of Electronics Engineering, Chungnam National University, Daejeon 34134, Republic of Korea*; orcid.org/0000-0001-7490-000X; Email: jaehyuk@cnu.ac.kr

Authors

Lee Kyung Bae − *Department of Electronics Engineering, Chungnam National University, Daejeon 34134, Republic of Korea*

Seong Gyun Son − *Department of Electronics Engineering, Chungnam National University, Daejeon 34134, Republic of Korea*

Sang-Chan Park − *Department of Electronics Engineering, Chungnam National University, Daejeon 34134, Republic of Korea*

Won Gyun Park − *Department of Electronics Engineering, Chungnam National University, Daejeon 34134, Republic of Korea*

Kiwan Kim − *Department of Electronics Engineering, Chungnam National University, Daejeon 34134, Republic of Korea*

Hyo-Ju Lee − *Department of Electronics Engineering, Chungnam National University, Daejeon 34134, Republic of Korea*

Daeun Bang − *Department of Electronics Engineering, Chungnam National University, Daejeon 34134, Republic of Korea*

Su-Ho Cho − *Korea National NanoFab Center (NNFC), Daejeon 34141, Republic of Korea*

Il-Suk Kang − *Korea National NanoFab Center (NNFC), Daejeon 34141, Republic of Korea*

Complete contact information is available at: https://pubs.acs.org/10.1021/acsomega.4c09156

Author Contributions

L.K.B., S.G.S., and J.H.A. conceived and designed the experiments. L.K.B., S.G.S., S.C.P., W.G.P., K.K., H.J.L., D.B., S.H.L., and I.S.K. fabricated the device. L.K.B. and S.G.S. performed the electrical measurements and data analysis. L.K.B., S.G.S., and J.H.A. organized the figures and wrote the manuscript. J.H.A. supervised the study. All authors approved the final version of the manuscript.

Notes

The authors declare no competing financial interest.

■ ACKNOWLEDGMENTS

This work was supported by research fund of Chungnam National University.

REFERENCES

(1) Novoselov, K. S.; Geim, A. K.; Morozov, S. V.; Jiang, D. E.; Zhang, Y.; Dubonos, S. V.; Firsov, A. A. Electric field effect in atomically thin carbon films. *Science* **2004**, *306* (5696), 666−669.

(2) Nair, R. R.; Blake, P.; Grigorenko, A. N.; Novoselov, K. S.; Booth, T. J.; Stauber, T.; Peres, N. M. R.; Geim, A. K. Fine structure constant defines the visual transparency of graphene. *Sci.* **2008**, *320* (5881), 1308.

(3) Lee, C.; Wei, X.; Kysar, J. W.; Hone, J. Measurement of elastic properties and intrinsic strength of monolayer graphene. *Sci.* **2008**, *321* (5887), 385−388.

(4) Jang, H.; Park, Y. J.; Chen, X.; Das, T.; Kim, M. S.; Ahn, J. H. Graphene-based flexible and stretchable electronics. *Adv. Mater.* **2016**, *28* (22), 4184−4202.

(5) Paton, K. R.; Varrla, E.; Backes, C.; Smith, R. J.; Khan, U.; O'Neill, A.; Conor, B.; Lotya, M.; Istrate, O. M.; King, P.; Higgins, T.; Barwich, S.; May, P.; Puczkarski, P.; Ahmed, I.; Moebius, M.; Pettersson, H.; Long, E.; Coelho, J.; O'Brien, S. E.; et al. Scalable production of large quantities of defect-free few-layer graphene by shear exfoliation of liquids. *Nat. Mater.* **2014**, *13* (6), 624−630.

(6) Ciesielski, A.; Samorì, P. Graphene via sonication assisted liquid-phase exfoliation. *Chem. Soc. Rev.* **2014**, *43* (1), 381−398.

(7) Berger, C.; Song, Z.; Li, X.; Wu, X.; Brown, N.; Naud, C.; Mayou, D.; Li, T.; Hass, J.; Marchenkov, A. N.; Conrad, E. H.; First, P. N.; de Heer, W. A. Electronic confinement and coherence in patterned epitope graphene. *Sci.* **2006**, *312* (5777), 1191−1196.

(8) Emtsev, K. V.; Bostwick, A.; Horn, K.; Jobst, J.; Kellogg, G. L.; Ley, L.; McChesney, J. L.; Ohta, T.; Reshanov, S. A.; Rohrl, J.; Rotenberg, E.; Schmid, A. K.; Waldmann, D.; Weber, H. B.; Seyller, T. Towards wafer-sized graphene layers by atmospheric-pressure graphitization of silicon carbide. *Nat. Mater.* **2009**, *8* (3), 203−207.

(9) Yu, Q.; Lian, J.; Siriponglert, S.; Li, H.; Chen, Y. P.; Pei, S. S. Graphene Segregated on Ni Surfaces and Transferred to Insulators. *Appl. Phys. Lett.* **2008**, *93* (11), 113103.

(10) Kwon, S. Y.; Ciobanu, C. V.; Petrova, V.; Shenoy, V. B.; Bareno, J.; Gambin, V.; Petrov, I.; Kodambaka, S. Growth of semiconducting graphene on palladium. *Nano Lett.* **2009**, *9* (12), 3985−3990.

(11) Coraux, J.; Diaye, N.; Busse, C.; Michely, T. Structural coherence of graphene on Ir (111). *Nano Lett.* **2008**, *8* (2), 565−570.

(12) Li, X.; Cai, W.; An, J.; Kim, S.; Nah, J.; Yang, D.; Piner, R.; Velamakanni, A.; Jung, I.; Tutuc, E.; Banerjee, S. K.; Colombo, L.; Ruoff, R. S. Large-area synthesis of high-quality and uniform graphene films on copper foils. *Science* **2009**, *324* (5932), 1312−1314.

(13) Bae, S.; Kim, H.; Lee, Y.; Xu, X.; Park, J. S.; Zheng, Y.; Balakrishnan, J.; Lei, T.; Kim, H. R.; Song, Y. I.; Kim, Y. J.; Kim, K. S.; Ozyilmaz, B.; Ahn, J. H.; Hong, B. H.; Iijima, S. Roll-to-roll production of 30-in. graphene films for transparent electrodes. *Nat. Nanotechnol.* **2010**, *5* (8), 574−578.

(14) Li, X.; Colombo, L.; Ruoff, R. S. Synthesis of graphene films on copper foils by chemical vapor deposition. *Adv. Mater.* **2016**, *28* (29), 6247−6252.

(15) Luo, D.; Wang, M.; Li, Y.; Kim, C.; Yu, K. M.; Kim, Y.; Han, H.; Biswal, M.; Huang, M.; Kwon, Y.; Goo, M.; Camacho, D. C.; Shi, H.; Yoo, W. J.; Altman, M. S.; Shin, H. J.; Ruoff, R. S. Adlayer-free large-area single crystal graphene grown on a Cu (111) foil. *Adv. Mater.* **2019**, *31* (35), No. 1903615.

(16) Li, X.; Zhu, Y.; Cai, W.; Borysiak, M.; Han, B.; Chen, D.; Piner, R. D.; Colombo, L.; Ruoff, R. S. Transfer of large-area graphene films for high-performance transparent conductive electrodes. *Nano Lett.* **2009**, *9* (12), 4359−4363.

(17) Kim, K. S.; Zhao, Y.; Jang, H.; Lee, S. Y.; Kim, J. M.; Kim, K. S.; Ahn, J. H.; Kim, P.; Choi, J. Y.; Hong, B. H. Large-scale pattern growth of graphene films for stretchable transparent electrodes. *Nat. Mater.* **2009**, *457* (7230), 706−710.

(18) Leong, W. S.; Wang, H.; Yeo, J.; Martin-Martinez, F. J.; Zubair, A.; Shen, P. C.; Mao, Y.; Palacios, T.; Buehler, M. J.; Hong, J. Y.; Kong, J. Paraffin-enabled graphene transfer. *Nat. Commun.* **2019**, *10* (1), 867.

(19) Qing, F.; Zhang, Y.; Niu, Y.; Stehle, R.; Chen, Y.; Li, X. Towards large-scale graphene transfer. *Nanoscale* **2020**, *12* (20), 10890−10911.

(20) Ullah, S.; Yang, X.; Ta, H. Q.; Hasan, M.; Bachmatiuk, A.; Tokarska, K.; Trzebicka, B.; Fu, L.; Rummeli, M. H. Graphene transfer methods: A review. *Nano Res.* **2021**, *14*, 3756−3772.

(21) Xue, X.; Mackin, C.; Weng, W. H.; Zhu, J.; Luo, Y.; Luo, S. X. L.; Lu, A. Y.; Hempel, M.; McVay, E.; Kong, J.; Palacios, T. Integrated Biosensor Platform Based on Graphene Transistor Arrays for Real-Time High-Accuracy Ion Sensing. *Nat. Commun.* **2022**, *13* (1), 5064.

(22) Wang, L.; Wang, X.; Wu, Y.; Guo, M.; Gu, C.; Dai, C.; Kong, D.; Wang, Y.; Zhang, C.; Qu, D.; Fan, C.; Xie, Y.; Zhu, Z.; Liu, Y.; Wei, D. Rapid and ultrasensitive electromechanical detection of ions, biomolecules, and SARS-CoV-2 RNA in unamplified samples. *Nat. Biomed. Eng.* **2022**, *6* (3), 276−285.

(23) Soikkeli, M.; Murros, A.; Rantala, A.; Txoperena, O.; Kilpi, O. P.; Kainlauri, M.; Sovanto, K.; Maestre, A.; Centeno, A.; Tukkiniemi, K.; Martins, D. G.; Zurutuza, A.; Arpiainen, S.; Prunnila, M. Wafer-scale graphene field-effect transistor biosensor arrays with monolithic CMOS readout. *ACS Appl. Electron. Mater.* **2023**, *5* (9), 4925−4932.

(24) Yılmaz, K.; Gürsoy, M.; Şakalak, H.; Ersöz, M.; Karaman, M. Transfer of CVD-Graphene on Real-World Surfaces in an Eco-Friendly Manner. *ACS Appl. Eng. Mater.* **2023**, *1* (8), 2042−2049.

(25) Shivayogimath, A.; Whelan, P. R.; Mackenzie, D. M.; Luo, B.; Huang, D.; Luo, D.; Wang, M.; Gammelgaard, L.; Shi, H.; Ruoff, R. S.; Boggild, P.; Booth, T. J. Do-it-yourself transfer of large-area graphene using an office laminator and water. *Chem. Mater.* **2019**, *31* (7), 2328−2336.

(26) Wang, Y.; Zheng, Y.; Xu, X.; Dubuisson, E.; Bao, Q.; Lu, J.; Loh, K. P. Electrochemical delamination of CVD-grown graphene film: toward the recyclable use of copper catalyst. *ACS Nano* **2011**, *5* (12), 9927−9933.

(27) Wang, M.; Huang, M.; Luo, D.; Li, Y.; Choe, M.; Seong, W. K.; Kim, M.; Jin, S.; Wang, M.; Chatterjee, S.; Kwon, Y.; Lee, Z.; Ruoff, R. S. Single crystal, large-area, fold-free monolayer graphene. *Nature* **2021**, *596* (7873), 519−524.

(28) Wang, H.; Yu, G. Direct CVD Graphene Growth on Semiconductors and Dielectrics for Transfer-Free Device Fabrication. *Adv. Mater.* **2016**, *28* (25), 4956−4975.

(29) Qian, F.; Deng, J.; Dong, Y.; Xu, C.; Hu, L.; Fu, G.; Chang, P.; Xie, Y.; Sun, J. Transfer-free CVD growth of high-quality wafer-scale graphene at 300 °C for device mass fabrication. *ACS Appl. Mater. Interfaces* **2022**, *14* (47), 53174−53182.

(30) Han, Y.; Park, B. J.; Eom, J. H.; Jella, V.; Ippili, S.; Pammi, S. V. N.; Choi, J. S.; Ha, H.; Choi, H.; Jeon, C.; Park, K.; Jung, H. T.; Yoo, S.; Kim, H. Y.; Kim, Y. H.; Yoon, S. G. Direct Growth of Highly Conductive Large-Area Stretchable Graphene. *Adv. Sci.* **2021**, *8* (7), No. 2003697.

(31) Hu, L.; Deng, J.; Xie, Y.; Qian, F.; Dong, Y.; Xu, C. In Situ Growth of Graphene on Polyimide for High-Responsivity Flexible PbS−Graphene Photodetectors. *Nanomaterials* **2023**, *13* (8), 1339.

(32) Park, B. J.; Choi, J. S.; Eom, J. H.; Ha, H.; Kim, H. Y.; Lee, S.; Shin, H.; Yoon, S. G. Defect-free graphene synthesized directly at 150 °C via chemical vapor deposition with no transfer. *ACS Nano* **2018**, *12* (2), 2008−2016.

(33) Lee, H.; Choi, T. K.; Lee, Y. B.; Cho, H. R.; Ghaffari, R.; Wang, L.; Choi, H. J.; Chung, T. D.; Lu, N.; Hyeon, T.; Choi, S. H.; Kim, D. H. Graphene-based electrochemical devices with thermoresponsive microneedles for diabetes monitoring and therapy. *Nat. Nanotechnol.* **2016**, *11* (6), 566−572.

(34) Kabiri Ameri, S.; Ho, R.; Jang, H.; Tao, L.; Wang, Y.; Wang, L.; Schnyer, D. M.; Akinwande, D.; Lu, N. Graphene electronic tattooing sensors. *ACS Nano* **2017**, *11* (8), 7634−7641.

(35) Kireev, D.; Kampfe, J.; Hall, A.; Akinwande, D. Graphene electronic tattoos 2.0, with enhanced performance, breathability, and robustness. *npj 2D Mater. Appl.* **2022**, *6* (1), 46.

(36) Zhang, H.; He, R.; Niu, Y.; Han, F.; Li, J.; Zhang, X.; Xu, F. Graphene-enabled wearable sensors for healthcare monitoring. *Biosens. Bioelectron.* **2022**, *197*, No. 113777.

https://doi.org/10.1021/acsomega.4c09156
ACS Omega 2025, 10, 1448−1456

(37) Huang, J.; Juszkiewicz, M.; De Jeu, W. H.; Cerda, E.; Emrick, T.; Menon, N.; Russell, T. Capillary wrinkling of floating thin polymer films. *Sci.* **2007**, *317* (5838), 650−653.
(38) Tang, X.; Yang, W.; Yin, S.; Tai, G.; Su, M.; Yang, J.; Shi, H.; Wei, D.; Yang, J. Controllable graphene wrinkles for a high-performance flexible pressure sensor. *ACS Appl. Mater. Interfaces* **2021**, *13* (17), 20448−20458.
(39) Afyouni Akbari, S.; Ghafarinia, V.; Larsen, T.; Parmar, M. M.; Villanueva, L. G. Large suspended monolayer and bilayer graphene membranes with diameter up to 750 μm. *Sci. Rep.* **2020**, *10* (1), 6426.
(40) Weidling, A. M.; Turkani, V. S.; Akhavan, V.; Schroder, K. A.; Swisher, S. L. Large-area photonic lift-off process for flexible thin-film transistors. *npj Flexible Electron.* **2022**, *6* (1), 14.
(41) Jinno, H.; Yokota, T.; Koizumi, M.; Yukita, W.; Saito, M.; Osaka, I.; Fukuda, K.; Someya, T. Self-powered flexible photonic skin for continuous biosignal detection via air-operation-stable polymer light-emitting diodes. *Nat. Commun.* **2021**, *12* (1), 2234.
(42) Kim, Y.; Suh, J. M.; Shin, J.; Liu, Y.; Yeon, H.; Qiao, K.; Kum, H. S.; Kim, C.; Lee, H. E.; Choi, C.; Kim, H.; Lee, D.; Lee, J.; Kang, J. H.; Park, B. I.; Kang, S.; Kim, J.; Kim, S.; Perozek, J. A.; Wang, K.; et al. Chipless wireless electronic skins using remote epitaxial freestanding compound semiconductors. *Science* **2022**, *377* (6608), 859−864.
(43) Ryu, J. *First-principles Study of Graphene Growth Mechanism on Oxide and Metal Substrates*. Ph.D. Thesis, Sejong University Graduate School: Republic of Korea, 2012.
(44) Seah, C. M.; Chai, S. P.; Mohamed, A. R. Mechanisms of graphene growth by chemical vapour deposition on transition metals. *Carbon* **2014**, *70*, 1−21.
(45) Bartelt, N. C.; McCarty, K. F. Graphene growth on metal surfaces. *MRS Bull.* **2012**, *37* (12), 1158−1165.
(46) Schroder, D. K. *Semiconductor material and device characterization*, 3rd ed.; Wiley & Sons: NJ, 2015.
(47) Giubileo, F.; Di Bartolomeo, A. Role of the contact resistance in graphene field-effect devices. *Prog. Surf. Sci.* **2017**, *92* (3), 143−175.
(48) Nagashio, K.; Nishimura, T.; Kita, K.; Toriumi, A. Metal/graphene contact as a performance killer of ultra-high-mobility graphene: analysis of intrinsic mobility and contact resistance. In *2009 IEEE International Electron Devices Meeting (IEDM)*, Baltimore, MD, USA, 2009; pp 1−4.
(49) Chen, S.; Brown, L.; Levendorf, M.; Cai, W.; Ju, S. Y.; Edgeworth, J.; Li, X.; Magnuson, C. W.; Velamakanni, A.; Piner, R. D.; Kang, J.; Park, J. W.; Ruoff, R. S. Oxidation resistance of graphene-coated Cu and Cu/Ni alloy. *ACS Nano* **2011**, *5* (2), 1321−1327.
(50) Krishnan, M. A.; Aneja, K. S.; Shaikh, A.; Bohm, S.; Sarkar, K.; Bohm, H. M.; Raja, V. S. Graphene-based anticorrosive coatings for copper. *RSC adv.* **2018**, *8* (1), 499−507.
(51) Lu, L. L.; Liu, H. T.; Wang, Z. D.; Lu, Q. Q.; Zhou, Y. J.; Zhou, F.; Song, K. X. Advances in electrolytic copper foils: fabrication, microstructure, and mechanical properties. *Rare Met.* **2024**, 1−36.
(52) Hong, N.; Kireev, D.; Zhao, Q.; Chen, D.; Akinwande, D.; Li, W. Roll-to-Roll Dry Transfer of Large-Scale Graphene. *Adv. Mater.* **2022**, *34* (3), No. 2106615.
(53) Li, J. T.; Stanford, M. G.; Chen, W.; Presutti, S. E.; Tour, J. M. Laminated Laser-Induced Graphene Composites. *ACS Nano* **2020**, *14* (7), 7911−7919.
(54) Zebrev, G. I.; Melnik, E. V.; Tselykovskiy, A. A. Interface traps in graphene field-effect devices: extraction methods and influence on characteristics. *arXiv* **2014**, 1405.5766.
(55) Coelho, B. J.; Pinto, J. V.; Martins, J.; Rovisco, A.; Barquinha, P.; Fortunato, E.; Baptista, P. V.; Martins, R.; Igreja, R. Parylene C as a multipurpose material for electronics and microfluidics. *Polymers* **2023**, *15* (10), 2277.
(56) Vanskeviče, I.; Kinka, M.; Banys, J.; Macutkevič, J.; Schaefer, S.; Selskis, A.; Fierro, V.; Celzard, A. Dielectric and ultrasonic properties of PDMS/TiO2 nanocomposites. *Polymers* **2024**, *16* (5), 603.
(57) Ayoub, E.; Dawaymeh, F.; Khaleel, M.; Alamoodi, N. Enhancing hydrophilicity of PDMS surfaces through graphene oxide deposition. *J. Mater. Sci.* **2024**, *59*, 8205−8219.
(58) Yavari, F.; Castillo, E.; Gullapalli, H.; Ajayan, P. M.; Koratkar, N. High sensitivity detection of NO_2 and NH_3 in air using chemical vapor deposition grown graphene. *Appl. Phys. Lett.* **2012**, *100* (20), 203120.
(59) Ji, H.; Zeng, W.; Li, Y. Gas sensing mechanisms of metal oxide semiconductors: a focus review. *Nanoscale* **2019**, *11* (47), 22664−22684.
(60) Das, S.; Jayaraman, V. SnO_2: A comprehensive review on structures and gas sensors. *Prog. Mater. Sci.* **2014**, *66*, 112−255.
(61) Singh, E.; Meyyappan, M.; Nalwa, H. S. Flexible graphene-based wearable gas and chemical sensors. *ACS Appl. Mater. Interfaces* **2017**, *9* (40), 34544−34586.
(62) Li, Z.; Li, H.; Wu, Z.; Wang, M.; Luo, J.; Torun, H.; Fu, Y. Advances in designs and mechanisms of semiconducting metal oxide nanostructures for high-precision gas sensors operated at room temperature. *Mater. Horiz.* **2019**, *6* (3), 470−506.
(63) Song, H.; Li, X.; Cui, P.; Guo, S.; Liu, W.; Wang, X. Sensitivity investigation for the dependence of monolayer and stacking graphene−NH3 gas sensors. *Diam. Relat. Mater.* **2017**, *73*, 56−61.
(64) Ko, G.; Kim, H. Y.; Ahn, J.; Park, Y. M.; Lee, K. Y.; Kim, J. Graphene-based nitrogen dioxide gas sensors. *Curr. Appl. Phys.* **2010**, *10* (4), 1002−1004.
(65) Xie, T.; Wang, Q.; Wallace, R. M.; Gong, C. Understanding and optimization of graphene gas sensors. *Appl. Phys. Lett.* **2021**, *119* (1), No. 013104.
(66) Kim, Y. H.; Kim, S. J.; Kim, Y. J.; Shim, Y. S.; Kim, S. Y.; Hong, B. H.; Jang, H. W. Self-activated transparent all-graphene gas sensor with endurance to humidity and mechanical bending. *ACS Nano* **2015**, *9*, 10453−10460.
(67) Peña, Á.; Matatagui, D.; Ricciardella, F.; Sacco, L.; Vollebregt, S.; Otero, D.; Horrillo, M. C. Optimization of multilayer graphene-based gas sensors by ultraviolet photoactivation. *Appl. Surf. Sci.* **2023**, *610*, No. 155393.
(68) Zhao, M.; Falak, A.; Tian, Y.; Yan, L.; Liu, R.; Chen, W.; Wang, H.; Wu, T.; Chen, P.; Chu, W. Cu/graphene interdigitated electrodes with various copper thicknesses for UV-illumination-enhanced gas sensors at room temperature. *Phys. Chem. Chem. Phys.* **2020**, *22* (44), 25769−25779.
(69) Barandun, G.; Gonzalez-Macia, L.; Lee, H. S.; Dincer, C.; Güder, F. Challenges and opportunities for printed electrical gas sensors. *ACS Sens.* **2022**, *7* (10), 2804−2822.
(70) Wang, T.; Huang, D.; Yang, Z.; Xu, S.; He, G.; Li, X.; Hu, N.; Yin, G.; He, D.; Zhang, L. A review on graphene-based gas/vapor sensors with unique properties and potential applications. *Nano-Micro Lett.* **2016**, *8*, 95−119.
(71) Steinhauer, S. Gas sensors based on copper oxide nanomaterials: A review. *Chemosensors.* **2021**, *9* (3), 51.
(72) Chen, H.; Zhuo, F.; Zhou, J.; Liu, Y.; Zhang, J.; Dong, S.; Liu, X.; Elmarakbi, A.; Duan, H.; Fu, Y. Advances in graphene-based flexible and wearable strain sensors. *Chem. Eng. J.* **2023**, *464*, No. 142576.
(73) Pang, J.; Peng, S.; Hou, C.; Zhao, H.; Fan, Y.; Ye, C.; Zhang, N.; Wang, T.; Cao, Y.; Zhou, W.; Sun, D.; Wang, K.; Rummeli, M. H.; Liu, H.; Cuniberti, G. Applications of graphene in the five senses, nervous system, and artificial muscles. *ACS Sens.* **2023**, *8* (2), 482−514.
(74) Peng, Z.; Chen, X.; Fan, Y.; Srolovitz, D. J.; Lei, D. Strain engineering of 2D semiconductors and graphene: from strain fields to band-structure tuning and photonic applications. *Light: Sci. Appl.* **2020**, *9* (1), 190.
(75) Yang, S.; Chen, Y. C.; Nicolini, L.; Pasupathy, P.; Sacks, J.; Su, B.; Yang, R.; Sanchez, D.; Chang, Y. F.; Wang, P.; Schnyer, D.; Neikirk, D.; Lu, N. Cut-and-Paste" manufacture of multiparametric epidermal sensor systems. *Adv. Mater.* **2015**, *27* (41), 6423−6430.
(76) Mahdavi, H.; Rahbarpour, S.; Goldoust, R.; Hosseini-Golgoo, S. M.; Jamaati, H. Investigating simultaneous effects of flow rate and chamber structure on the performance of metal oxide gas sensors. *IEEE Sens. J.* **2021**, *21* (19), 21612−21621.

https://doi.org/10.1021/acsomega.4c09156
ACS Omega 2025, 10, 1448−1456